# Fracture mechanics and reliability of rupture of cast iron rotating disc

**Haider Hadi Jasim**
**Assist.Lecut.in Chemical Engineering**
**Basrah University,**

## Abstract

***In this paper, the crack propagation in opening mode (Mode I) for three kinds of cast iron rotating disc: Flake graphite cast iron disc, Compacted Vermicular cast iron disc, and Spheroidal graphite cast iron disc are analysed by using Boundary Element Method (BEM) and Finite Element Method (FEM). Weibull uni-axial and multi-axial distribution function is developed and applied to evaluate the reliability of the fracture strength of rotating cast iron disc have inner surface crack. As a result the stress intensity factor ($K_I$) for Flake graphite disc (FGD) is smallest, while ($K_I$) for Spheroidal graphite disc (SGD) was the larger, the value of ($K_I$) for Compacted Vermicular disc (CVD) has intermediate between the two cast iron discs. It is found that there is a convergence between results obtained from uni-axial and multi-axial distribution function, but multi-axial distribution function give high values compared to uni-axial distribution function.***

***Key words: Stress intensity factor, rotational loading, finite element method, boundary element method.***

## 1- Introduction

Cast iron rotating disc is used in many applications such as electrical generator, flywheel on diesel engine, … etc., where centrifugal force is very important and may caused failure.

In general there are three kinds of cast iron used in manufacturing rotating disc according to form of graphite exists: Spheroidal graphite cast iron, in this kind the graphite exist in nodular form, Compacted Vermicular cast iron, in this kind the graphite exist on rosettes form, and Flake graphite cast iron, in this kind the graphite exist on flake form [1].

The presence of crack in cast iron disc reduces the fatigue and static strength because the stresses and strains are highly magnified at the crack tip. The use of parameter to describe the local stresses and strains magnification at crack tip is important to evaluation cast iron disc integrity. This parameter is called stress intensity factor.

There are more studies on cast iron disc most of them focused on fatigue. Shikida M. [2], steady about fatigue crack propagation in cast iron disc using analytical and experimental approaches. Yotaro Mutsuo [3] developed a new distribution function to expected values of the rupture strength of brittle rotating disc. Luciano M. Bezerra [4], use boundary element method and finite element method for calculation of the stress intensity factor in opening mode in two-dimensional plate has central crack.

In this paper the $J$ – Integral programs with finite element method and boundary element method are developed and used for analysis of cast iron disc under rotational loading, and thermal loading. Weibull model is used in analysis of cast iron disc by using uni-axial and multi-axial distribution function to evaluate the reliability of disc. The steady is focused on bi-dimensional elastic and a plain strain condition.

## 2– Developing of Governing Equations

The use of numerical method such as boundary element method (BEM) and finite element method (FEM) is economical tool for consuming time. In the following sections, describe the FEM and BEM technique used.

### A) Finite Element Method.

The finite element method (FEM) is a numerical techniques for obtain approximate solution to a wide variety of the engineering problems.

The procedure used can be simulating by using displacement method as followers [5, 6]:

**Step 1:**

The generalized equilibrium equation for linear situation can be expressed as follows:

$$\iiint B^t \, \sigma \, dv = F \tag{1}$$

Where,
B: Strain – displacement matrix.
$\sigma$: Stress vector.
F: Force vector.

**Step 2:**

The whole domain is divided into finite element, which is connected together by specific nodes. Then the displacement vector $\underline{U}$ at point (x, y) can be expressed as follows:

$$\underline{U}(x,y)=\sum_{i=1}^{n}u_i N_i(x,y) \quad (2)$$

$N_i(x,y)$ : Element shape function.

$n$ : Number of nodes.

**Step 3:**

The relation between the applied force acting on the nodes and the nodal displacement can be expressed by using which called element stiffness matrix as follows:

$$K_e=\iint \underline{B}^t \underline{D}\, B\, dxdy \quad (3)$$

where,

$\underline{D}$: D- matrix (matrix contain the element properties such as modulus of elasticity and Poisson's ratio).

**Step 4:**

The nodal stiffness and nodal loads for each of the element sharing the same nodes are add to each other to obtain the net stiffness and the net load at the specific nodes, so the global matrix can be expressed as:

$$\underline{K}=\sum_{e=1}^{ne}\underline{K}_{(e)} \quad (4)$$

$$P=\sum_{e=1}^{ne}\underline{P}_{(e)} \quad (5)$$

$\underline{K}_{(e)}$ : Element stiffness matrix.

$\underline{P}_{(e)}$ : Element force vector.

$ne$ : Number of element.

**Step 5:**

The overall system of equation of the domain can be written as:

$$[\,K\,]\,[\,U\,]=[\,P\,] \quad (6)$$

Where,

[U]: Global displacement vector.

In order to solve the above system of equations, the following boundary conditions are applied:

1- At loaded nodes the displacement is unknown and the applied force is known.

2- At supported nodes the load is unknown and the displacement is known.

**Step 6:**

**A-** The body force (rotating loads) for any node in element is derived as followers [7]:

For a uniform rotating about (Z-axis), the node (i) rotating load is given by:

$$F_{xi}=[\iint tN_i dA]Q_{xi} \quad (7)$$

$$F_{yi}=[\iint tN_i dA]Q_{yi} \quad (8)$$

and,

$$Q_{xi}=-\rho(x-x_o)\omega^2$$

$$Q_{yi}=-\rho(y-y_o)\omega^2$$

where,

$N_i$ : Shape function

$t$ : Thickness of disc (m)

$\rho$ : Density (kg / m$^3$)

$\omega$ : Angular velocity in (rad /s)

$F_{xi}$ : Nodal rotation load in x-direction

$F_{yi}$ : Nodal rotation load in y-direction.

**B-** When structure is exposed to a steady state linear temperature distribution T(x, y) the thermal loading vector is:

$$\underline{F}=\underline{F}^o_\varepsilon+\underline{F}^o_\sigma \quad (9)$$

$$\underline{F}^o_\varepsilon=+\iint_{element} t\underline{B}^t\underline{D}\ \underline{\varepsilon}^o dxdy$$

$$\underline{F}^o_\sigma=-\iint_{element} t\underline{B}^t\underline{D}\ \underline{\sigma}^o dxdy$$

**Step 7:**

The system of equation can be solving using Gauss-elimination solver to determine the displacement at each node. Then the strain and stress at each element can be calculating by using strains-displacement and stress – strain relation as follows:

$$\left.\begin{array}{l}\varepsilon=\underline{BU}\\ \underline{\sigma}=\underline{D}\varepsilon\end{array}\right\} \quad (10)$$

where,

$\underline{\sigma}$ : Stress vector.

$\underline{\varepsilon}$ : Strain vector.

**B) Boundary Element Method**

Boundary element method (BEM) has emerged as a powerful numerical method, which has certain advantages over the finite element method. The (BEM) is particular suited to cases where better accuracy is required due to problems such as stress concentration and rotational loading or where the domain of interest extends to infinity [8].

By using Betti's Reciprocal theorem [4], an equivalent integral equation can be obtained and then converted to a form that involves surface integral, i.e. over the boundary. The boundary is divided into element and selection a node along the boundary.

Hasiao G. C. [9] give the general governing integral equation for two-dimensional elastic disc and by using weighted residual method for the point ( i ) as follows:

$$u_l^i = -\int_{\Gamma} T^*_{lk} u_k d\Gamma + \int_{\Gamma} u^*_{lk} T_k d\Gamma + \int_{\Omega} u^*_{lk} b_k d\Omega + \int_{\Gamma} \left[S_i \Delta T - V_i \frac{\partial T}{\partial n}\right] d\Gamma + \int Q_i d\Gamma \quad (11)$$

and,

$$T_{lk} = \frac{-1}{4\pi(1-\pi)r}\left\{ \frac{\partial r}{\partial n}[(1-2\nu)\delta_{lk} + 2r,_k\, r,_l\,] + (1-2\nu)(n_l r,_k - n_k r,_l) \right\}$$

$$\overset{*}{u}_{lk} = \frac{1}{8\pi\mu(1-\nu)} * [(3-4\nu)\ln\frac{1}{r}\delta_{lk} + r,_l\, r,_k\,]$$

$$r,_l = \frac{\partial r}{\partial x}, \quad r,_k = \frac{\partial r}{\partial y}$$

$$S_i = \frac{-\alpha(1+\nu)}{4\pi(1-\nu)}\left[\left(\ln(r) + \frac{1}{2}\right)n_i + \frac{\partial r}{\partial n} r,1\right]$$

$$V_i = \frac{-\alpha(1+\nu)}{4\pi(1-\nu)}\left[\left(\ln(r) + \frac{1}{2}\right) r,_1\, r\right]$$

where,

$u_l^i$ : Displacement at node i

$T_{lk}$ and $u_{lk}$ : Traction and displacement at any point in the (k) direction when a unit load is applied at node ( i ) in the ( l ) direction.

$T_k$ and $u_k$ : Traction and displacement at a point in the domain for the point load considering each direction as independent.

$\Omega$ : Domain of disc.

$\nu$ : Poisson's ratio

$r_{,l}$ and $r_{,k}$ : Represent the radius derivatives with respect to (x) and (y) direction respectively.

$n$ : Unit vector normal to the outer boundary of the body.

r: Distance between the load point and the field point.

$\mu$ : Shear modulus.

$b_k$ : Body force.

The body force treatment as followers [9, 10]:
For a body force in the x-direction:

$$\int_{\Omega} u_{lk} b_k d\Omega = \int_{\Omega} (u_x b_x + u_{xy} b_y) d\Omega \quad (12)$$

and the body force in the y-direction:

$$\int_{\Omega} u_{lk} b_k d\Omega = \int_{\Omega} (u_{xy} b_x + u_u b_y) d\Omega \quad (13)$$

where,

$$b_x = \rho(x - x_o)\omega^2$$

$$b_y = \rho(y - y_o)\omega^2$$

$$u_x = \Delta^2 G - \frac{1}{2(1-\nu)}\frac{\partial^2 G}{\partial x^2}$$

$$u_{xy} = -\frac{1}{2(1-\nu)}\frac{\partial^2 G}{\partial x \partial y}$$

$$u_y = \Delta^2 G - \frac{1}{2(1-\nu)}\frac{\partial^2 G}{\partial y^2}$$

$$G = \frac{1}{8\rho\mu} r^2 \ln \frac{1}{r}$$

$$r = x_{i+1} - x_i$$

and,
G: Galerkin function.
$x_o$ and $y_o$ : Center rotation of disc.
i: Represent node i.

Using the discredited form of eq. 10, the displacement $u_i$ at any point on the boundary can be calculated. With the displacement, the strains can be calculated, and with the strains, making use Hook's law, the stresses at any point calculated.

**C) Stress Intensity Factor and J-Integral Approach**

There are three types of stress intensity factor modes: opening mode (mode I) with $K_I$ parameter, shear mode (mode II) with $K_{II}$ parameter and mixed mode (mode III) with $K_{III}$ parameter. Among them mode I with $K_I$ parameter is the most important to know because $K_I$ characterize the stress field in the neighborhood of a crack tip when the crack under tension.

The J-Integral is an attractive parameter to characterize crack tip condition. It is a convenient method for computing the energy release rate associated with the extension of crack.

The $J$ - Integral equation is given by Kishimoto and Aoki in the form [5]:

$$J = \int_{\Gamma} w dy - \int_{\Gamma} T_r \frac{\partial u_i}{\partial x} ds + \iint_{\Omega} F \frac{\partial u_i}{\partial x} dx dy + \iint_{\Omega} \alpha \sigma_{ij} \frac{\partial T}{\partial x} dx dy \qquad (14)$$

where,
W: Strain energy per unit volume.
$u_i$ : Displacement vector.
F: Body force (rotational loading).
$T_r$ : Traction vector.
$dx$ and $dy$ : Infinitesimal element along the x-direction and y-direction
$ds$ : Infinitesimal distance on the path S.
$\alpha$ : Coefficients of thermal expansion of disc material.
T: Temperature distribution.

The J-Integral related to the stress intensity factor in the opening mode (mode I) by the following equation:

$$J = \frac{K_I^2}{E'} \qquad (15)$$

where,

$E' = E$ for plain stress.

$E' = \dfrac{E}{1 - \nu^2}$ for plain strain.

E: Modulus of elasticity.

Fig.1-A shows the geometry of the disc specimen. The inside diameter and outside diameter of a disc are 20 mm and 200 mm respectively. The disc contain double edge internal crack. The disc specimen has same dimensions for three types of cast iron materials used in analysis.

Fig. 1B shows an example of finite element division by using a total 200 element with nine-node isoperimetric elements were used, and the boundary element divisions by using a total 40 elements were employed.

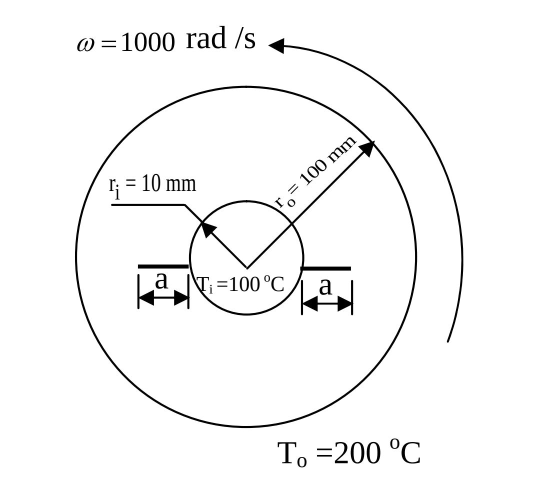


**A-Disc specimen.**

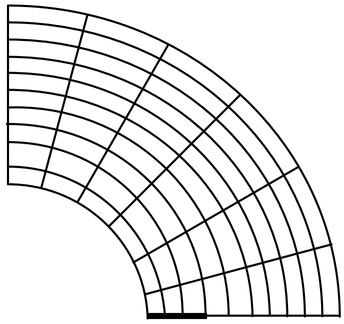

**B- Finite element meshes**

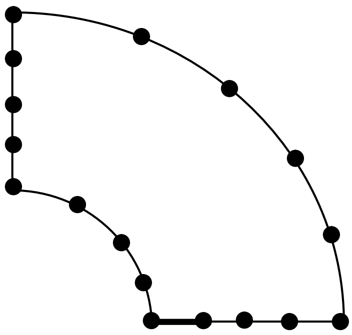

**C- Boundary element mesh.**

**Fig.1** Disc specimen and example of FEM and BEM mesh.

Tables 1 and Table 2 show their chemical composition and mechanical properties for discs materials

**Table1.** Chemicals compositions of material disc used.

| Chemical Composition Wt % | Materials | | |
|---|---|---|---|
| | FGD | CVD | SGD |
| C | 3.24 | 3.80 | 3.57 |
| Si | 2.31 | 2.55 | 2.68 |
| Mn | 0.358 | 0.445 | 0.314 |
| P | 0.025 | 0.023 | 0.022 |
| S | 0.008 | 0.010 | 0.012 |
| Mg | ---- | 0.016 | 0.042 |

**Table2**. Mechanical properties and percentage of carbon contained for three types of disc materials.

| Constants | Materials | | |
|---|---|---|---|
| | Flake graphite | Compacted Vermicular | Spheroidal graphite |
| E (GPa) | 90 | 142 | 163 |
| $\sigma_t$ (MPa) | 145 | 334 | 293 |
| $\gamma$ | 0.2 | 0.25 | 0.26 |
| $\rho$ (kg / m$^3$) | 7180 | 7300 | 7640 |
| $\mu$ (GN/m$^2$) | 41 | 91 | 185 |
| m | 9.2 | 9.2 | 9.2 |
| $m_2$ | 2.51 | 2.405 | 2.42 |

## 4- Weibull Analysis

The key element in the design and fabrication of a component pertains it is reliability (usually determined by a safety or economic consideration), it is important to know the statistical probability of a given fracture event. According to Weibull, the two parameter distribution function $S(B_o)$ when a body subjected to a uni-axial tensile stress ($\sigma$) is given by [3] :

$$S(B_o) = e^{-B_o\left(\frac{\sigma-\sigma_u}{\sigma_o}\right)^m} \qquad (16)$$

where,

S ($B_o$): Probability of survive.

$B_o$: Volume or surface area of a body. $\sigma$: Applied stress,

$\sigma_u$: Stress below which there is a zero probability of failure.

$\sigma_o$ : Mean strength of material

$m$ : Weibell modulus.

For brittle material $\sigma_u = 0$.

The risk of rupture (R) is given by the following equation:

$$R = 1 - e^{-B_o\left(\frac{\sigma}{\sigma_o}\right)^m} \qquad (17)$$

Weibull also has a heuristically obtained the following multi-axial distribution function by taking the direction of the cracks at every point in the body into account for multi-axial stress state

( $\sigma_1, \sigma_2, \sigma_3$ ) as shown in Fig.1 [6]:

$$R = 1 - e^{-\int_V (K \int_A \sigma_n^m \, dA) dV} \qquad (18)$$

where,

$\sigma_n$ : Normal stress on the crack plane and is given by:

$$\sigma_n = \cos^2\phi(\sigma_1 \cos^2\varphi + \sigma_2 \sin^2\varphi) + \sigma_3 \sin^2\phi \qquad (19)$$

$dA$ : Area element of the unit sphere.

$dV$ : Volume element of unite sphere.

$\varphi$ and $\phi$ : Angle between crack and coordinates.

K: Parameter constant and is given by:

$$K = \left( \beta \sigma_o^m 2 \right)^{-1} \qquad (20)$$

$\beta$ : Beta function.

$m_2$ : Weibull parameter.

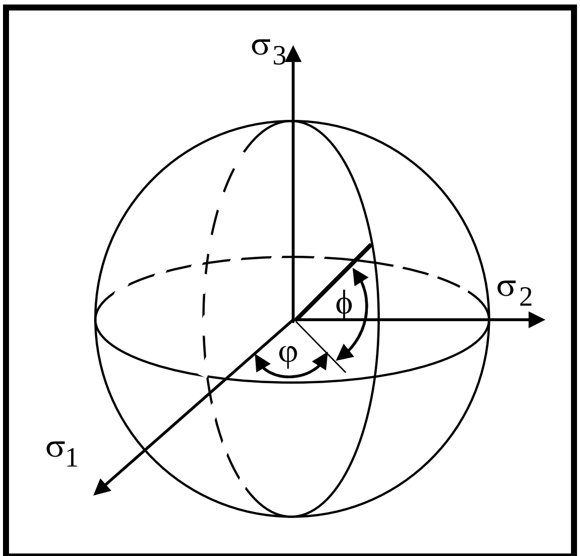


**Fig.2** Unit sphere.

**5- The Expected Rupture Strength of Cast Iron Disc Under Rotation Loading.**

For a hollow cast iron disc rotating at angular velocity ( $\omega$ ), the circumferential stress ( $\sigma_t$ ) and radial stress ( $\sigma_r$ ) are given by [11]:

$$\sigma_t = \frac{\rho\omega^2}{8}[(3+\nu)(R_i^2 + R_o^2 + \frac{R_i^2 R_o^2}{r^2}) - (1+3\nu)r^2] \qquad (21)$$

$$\sigma_r = \frac{\rho\omega^2}{8}(3+\nu)(R_i^2 + R_o^2 - \frac{R_i^2 R_o^2}{r^2} - r^2) \ldots \qquad (22)$$

where,

$R_i$ : Inner radius of disc.

$R_o$ : Outer radius of disc.

Since $\sigma_t > \sigma_r$ at any radius in the disc, and maximum circumference stress occurs at inner radius then, the maximum stress ( $\sigma_{max.}$ ) is given by:

$$\sigma_{max.} = (\sigma_t)_{r=R_i}$$

$$\sigma_{max} = \frac{\rho\omega^2}{4}[(3+\nu)R_o^2 + (1-\nu)R_i^2)] \qquad (23)$$

In the following sections, propose risk of rupture by using distribution functions described in eq.17 and eq.18.

**A-** In the case of taking only internal cracks into consideration (uni-axial distribution function), for a hollow disc, defining the function $f_1(r)$ is:

$$f_1(r) = \frac{\sigma_t}{\sigma_{max.}}$$

$$f_1(r) = \frac{(R_o^2 + R_i^2 + \frac{R_o^2 R_i^2}{r^2}) - \frac{(1+3\nu)r^2}{(3+\nu)}}{2(R_o^2 + \frac{(1-\nu)}{(3+\nu)} R_i^2)} \qquad (24)$$

and,

$$R(\sigma_{max}) = 1 - e^{-B_o (\frac{\sigma_{max}}{\sigma_o})^m} \qquad (25)$$

where,

$$B_o = 2\pi h \int_{R_i}^{R_o} f(r)^m \, r dr \qquad (26)$$

$h$ : Thickness of disc.

**B-** In the case of taking only internal cracks into consideration (multi-axial distribution function), defining $f_2(r)$ in a hollow disc as:

$$f_2(r) = \frac{\sigma_r}{\sigma_{max}}$$

$$f_2(r) = \frac{(R_o^2 + R_i^2 - \frac{R_o^2 R_i^2}{r^2}) - \frac{r^2}{(3+\nu)}}{2(R_o^2 + \frac{(1-\nu)}{(3+\nu)} R_i^2)} \quad (27)$$

and,

$$R(\sigma_{max}) = 1 - e^{-B_1 K (\frac{\sigma_{max}}{\sigma_o})^m} \quad (28)$$

where,

$$B_1 = \Phi \int_{R_i}^{R_o} \int_0^{\frac{\pi}{2}} [f_1(r)\cos^2\varphi + f_2(r)\sin^2\varphi]^m \, r d\varphi dr \quad (29)$$

where,

$$\Phi = \frac{4\pi h}{\beta(m + \frac{1}{2}, \frac{1}{2})}$$

$$\beta(\chi, \lambda) = \int_0^1 x^{\chi-1}(1-x)^{\lambda-1} dx$$

$\beta$ : Beta functions.

$\chi$ and $\lambda$ : Are constants and $\chi > 0$, $\lambda > 0$.

## 4- The Expected Rupture Strength of Cast Iron Disc Under Rotation and Thermal Loading.

For a hollow disc subjected at inner surface to temperature $T_i$ and outer surface to temperature $T_o$, and for steady state heat flow, the temperature distribution through disc is given by [7]:

$$r\frac{dT}{dr} = c$$

$$\frac{dT}{dr} = \frac{c}{r}$$

$$T = b\ln(r) + a \quad (30)$$

where,
a and b: Constants

The radial and tangential stresses are given by the following equations [11]:

$$\sigma_r = A - \frac{B}{r^2} - \frac{E\alpha T}{2(1-\nu)} - (3+\nu)\frac{\rho\omega^2 r^2}{8} \quad (31)$$

… (31)

$$\sigma_t = A + \frac{B}{r^2} - \frac{E\alpha T}{2(1-\nu)} - \frac{E\alpha b}{2(1-\nu)} - (1+3\nu)\frac{\rho\omega^2 r^2}{8} \quad (32)$$

where,
E: Modulus of elasticity.
$\alpha$ : Coefficient of thermal expansion.
A and B are constants determine from condition $\sigma_r = 0$ at $r = R_i$ and $r = R_o$

The maximum stress occurs at inner radius and given by equations:

$\sigma_{max.} = \sigma_t$ at $r = R_i$

$$\sigma_{max} = \frac{E\alpha}{(1-\nu)(R_i^2 - R_o^2)}(T_i - T_o) + \frac{(3+\nu)}{4}\rho\omega^2 R_i^2 (R_o^2 + 2) + \frac{E\alpha T_i}{(1-\nu)} + \frac{E\alpha b}{(1-\nu)} - \frac{(1+3\nu)}{8}\rho\omega^2 R_i^2$$

The distribution function for uni-axial and multi-axial distribution is given as before by [2]:

$$f_1(r) = \frac{\sigma_t}{\sigma_{max}} \quad \text{and} \quad f_2(r) = \frac{\sigma_r}{\sigma_{max}}$$

Then can be used eq.26 for uni-axial and eq.29 for multi-axial distribution to determine the risk of rupture under rotation and thermal loading at different point along radius of disc.

## 6-The Expected Value of the Fracture Rotating Speed

The expected values of ($\sigma_{max.}$) for fracture of hollow disc can be obtained from the following equation [4]:

$$E(\sigma_{max}) = \int_0^{\infty} (1 - R(\sigma_{max}))d\sigma_{max} \quad (33)$$

The expected values of ($\omega^2$) which fracture occurs in uni-axial and multi-axial distribution function is given by:

$$E(\omega^2) = \frac{4}{\rho((3+\nu)R_o^2 + (1-\nu)R_i^2)} * E(\sigma_{max.}) \quad (34)$$

## 7– Result and Discussion

Fig.3 shows the J-Integral values for each crack length to width ratios (difference between outer and inner radius) for the three types of cast iron disc. These values were calculated for 9 to 45 mm long crack by means of the FEM and BEM. As illustrated in the figure, the J-values increase with increase creak length to width ratio due to increase of stress concentration at the creak tip.

Based upon the numerical results of stress intensity factor presented in Fig.4, which shows $K_I$ vs. crack length to width ratios for three kinds of disc specimens. It can be observe that there are good agreements between (FEM) and (BEM) results.

As indicated the value of $K_I$ for flake graphite disc is smallest, the value of $K_I$ for Spheriodal graphite disc is the largest and Compacted Vermicular graphite has intermediate value between them. This attributed to the difference in the material constant especially modulus of elasticity of three kinds of cast iron disc materials used for analysis.

Figs.5, 7, and 9 shows the risk of rupture (probability of failure) for the three types of disc under rotation loading and thermal loading. The curves are obtained by drawing the risk of rupture obtained from eq.26 and eq.27. The curves show there is a good agreement between them. As indicated, the risk of rupture increases with increasing radius because of increasing crack length.

Figs. 6, 8, and 10 shows the expected values of rupture of rotating speed against radius. It can be seen the fracture speed decrease with increasing radius. This attributed to that the crack focused stresses at inside zone of disc material and make it weakest and this lead to reduce the strength of disc material, therefore the expected values of fracture speed is decreased.

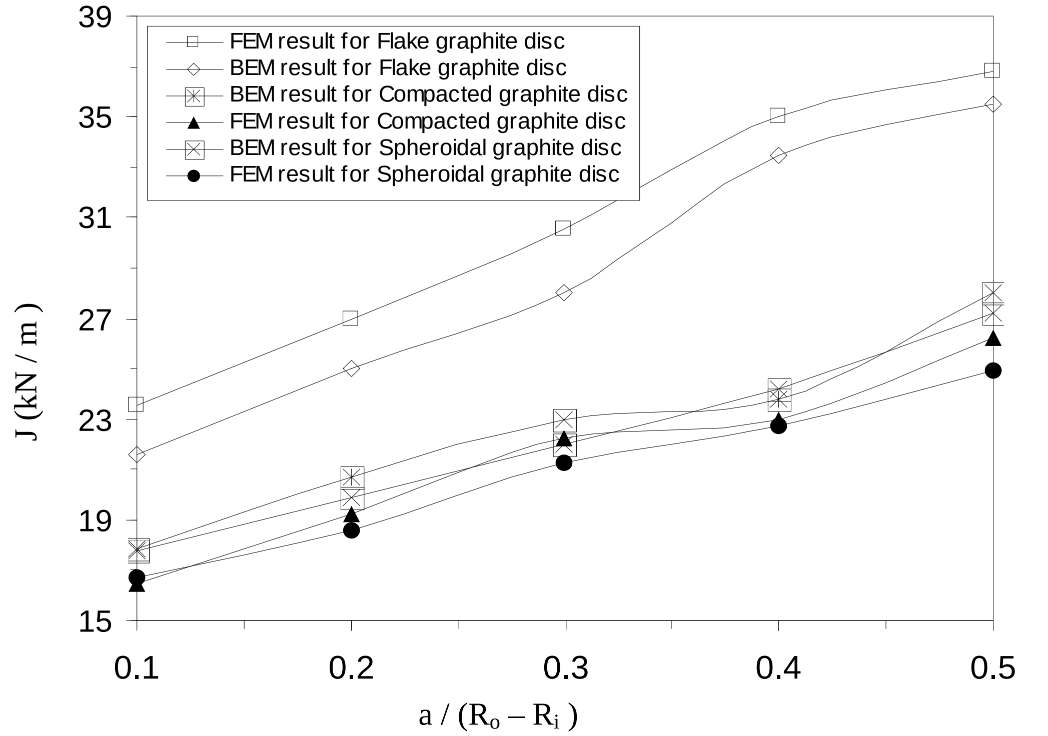


**Fig.3** J-values at different crack to width ratio for the three types of cast iron disc.

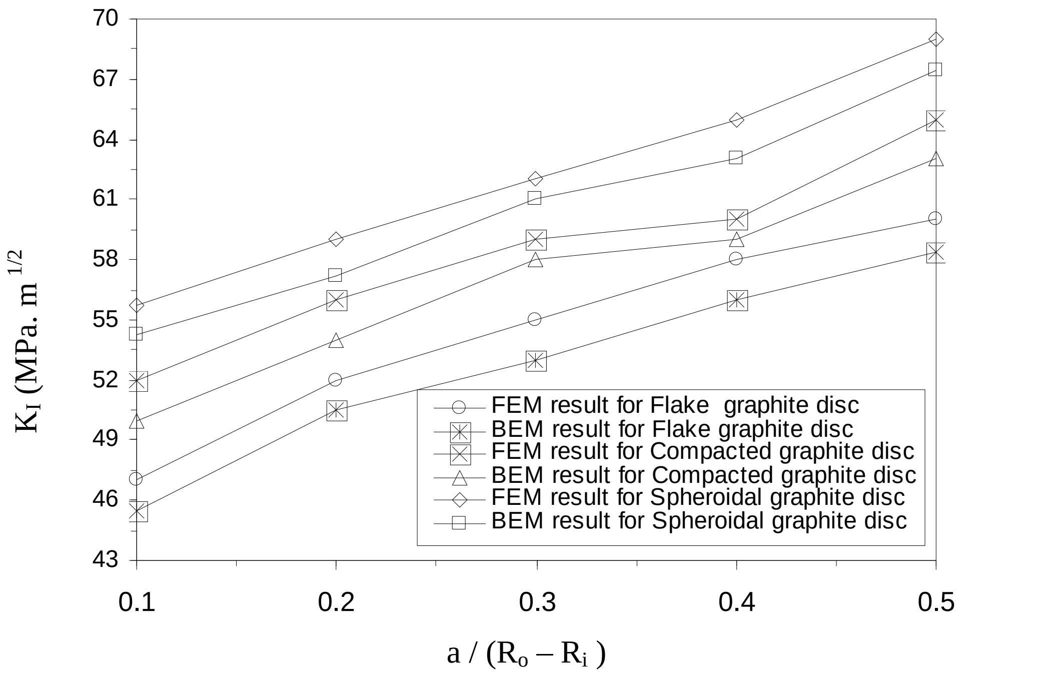


**Fig.4**. $K_I$ values at different crack length to width ratio for three types of cast iron disc.

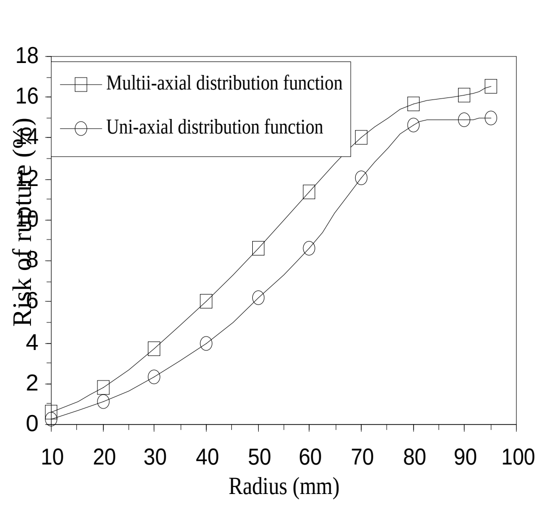


**Fig.5** Risk of failure for Flake graphite cast iron disc.

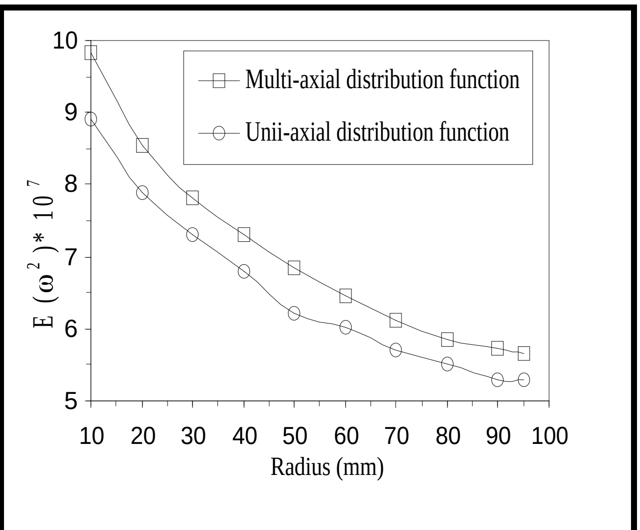


**Fig.6** Expected values of $\omega^2$ for Flake graphite cast iron disc.

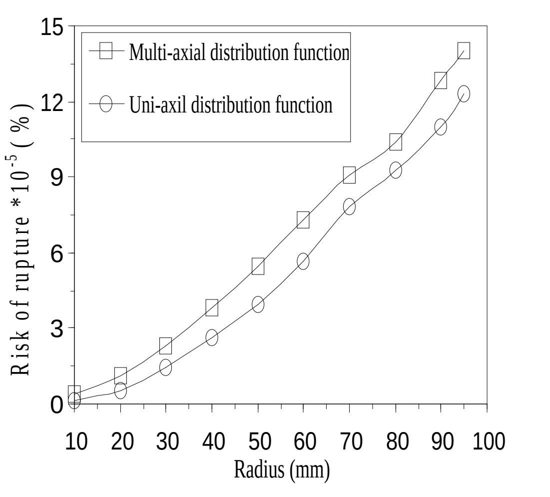


**Fig.7** Risk of rupture for Compacted Vermicular graphite cast iron disc.

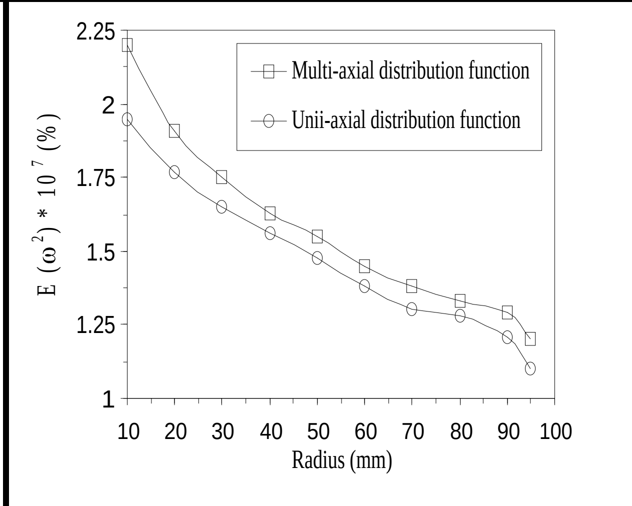


**Fig.8** Expected values of $\omega^2$ for Compacted graphite cast iron disc.

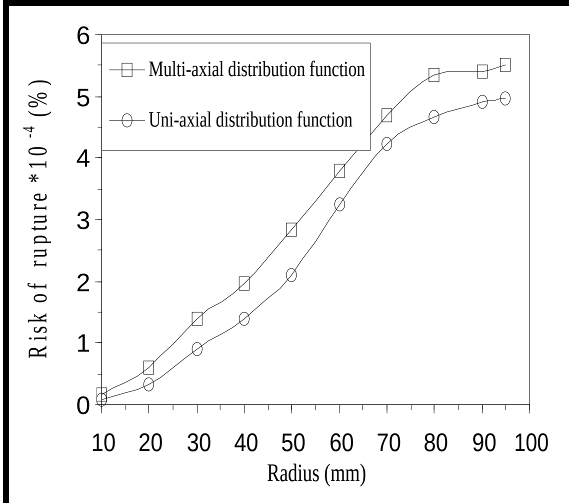


Fig.9 Risk of rupture for Spheroidal graphite cast iron disc.

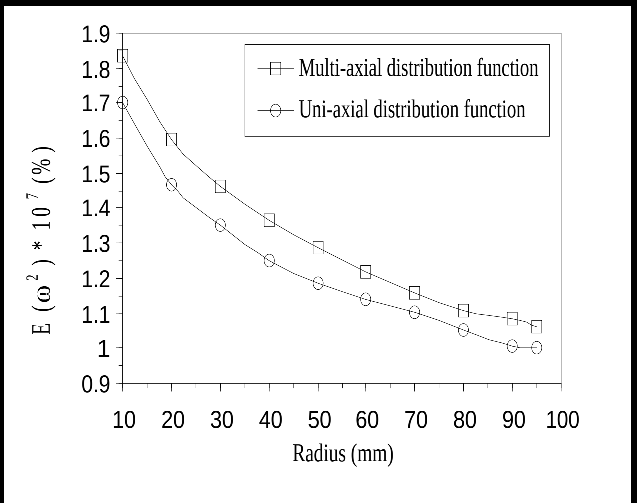


**Fig.10** Expected values of $\omega^2$ for Spheroidal graphite cast iron disc.

## 8 Conclusions

Based on the preceding studies, the following conclusions are reaches:

1- A comparative boundary element and finite element techniques has been carried out to calculate stress intensity factor in opening mode (mode I) within three kinds of cast iron disc specimens of linear elastic fracture mechanics.

2- An increase in the crack length will cause an increase in the stress intensity factor results from increasing stresses on crack tip.

3-Weibull uni-axial and multi-axial distribution function is applied in cast iron wheel taking the effect of existing crack.

4- The expected rupture of rotating speed under the combined effect of both rotational and thermal loading in cast iron disc is analyzed.

**Acknowledgment**

The author expresses thanks to Dr. I. R. Kamal the former head of chemical engineering department and all staff in the chemical engineering department.

## 9 References

[1] Bolton W. “Engineering material technology” Butterworth Heinemann Inc. England, (1999).

[2] Shikida M., et al. ‘‘Fatigue crack propagation for cast iron rotating disk’, JSME International Journal Series A, vol. 38, no. 1, 1995.

[3] Yotaro Matsuo and Hideyuki Sato “A probabilistic treatise of rupture of brittle rotating disc”, Bulletin of the JSME, Vo.22, No.172, 1989.

[4] Luciano M. Berzerr, Jaqueline M.S. de mederiors, Franco G. Cesari, and Paolo Battistela “ Using boundary element and j-integral for the determination of $K_I$ in fracture mechanics”, Report of LABEM International association for boundary element methods, UT Austin TX,USA , 2002.

[5] Takeuch N., Kishmoto K., Aoki S., and M. Sakta, “Study On the accuracy of J-Integral calculation by finite element method”, The ASME Pressure Vessels and Piping Conferences PVP, vol. 160, 1989.

[6] Chen W. H. and TA-Chyan Lin, “Mixed – mode crack analysis of rotating disk using finite Element methods”, International Journal of Science and Engineering, Vol.16, 1983.

[7] Salah N. A., “Domain loading fracture mechanics analysis linear analysis using finite element method” M.Sc. Thesis, Basrah University, 1996.

[8] Dretta E, Francissco J. S., and Rossana V., “The variational indirect boundary element method: A strategy toward the solution of very large problems of site response”, J. of computational a caustics, vol.9, no. 2, pp. 531-541, 2001.

[9] Hasiao G. C. and Wendland L. “Boundary element method foundation and error analysis”, Encyclopedia of computational mechanics, Johan Wiley and sons, 2004.

[10] Gospodin Gospodinov “Boundary element modeling of cohesive crack using displacement discontinuity method”, Section one, fracture mechanics, Advance in boundary element method, Ed. R. Gallegoand and M. H. Aliabadi, 2003.

[11] Hearn E. J., “Mechanics of Material”, Pergamon International Library, 1979.

# ميكانيك الفشل واحتمالية الانهيار للاقراص الدورانه المصنعة من حديد الصب

**حيدر هادي جاسم**

**مدرس مساعد**

**قسم الهندسة الكيمياوية**

**كلية الهندسة/ جامعة البصره**

## الخلاصة:

في هذا البحث، انتشار الشق في حالة النمط المفتوح (Mode I) لثلاثة أنواع من أقراص الحديد الدوارة، قرص مصنوع من حديد الزهر ذو الكرافيت ألشرائحي أو ( القشري) ، قرص مصنوع من حديد الزهر ذو الكرافيت المتكور، وقرص مصنوع من حديد الزهر ذو الكرافيت ألنجمي المدمج ، تم دراستها وتحليلها باستخدام طريقة العناصر الحدودية (BEM) وطريقة العناصر المحددة (FEM) . طبقت دوال ويبل متعددة التوزيع للإبعاد من اجل حساب احتمالية الفشل واحتمالية مقاومة الانكسار للقرص الدوار الذي يحتوي على شق داخلي. لقد وجد إن معامل شدة الإجهاد ($K_I$) للقرص المصنوع من حديد الزهر ذو الكرافيت ألشرائحي ( القشري) هو الأصغر، بينما معامل شدة الإجهاد ($K_I$) للقرص المصنوع من حديد الزهر ذو الكرافيت ألنجمي الاعتيادي هو الأكبر، وان معامل شدة الإجهاد ($K_I$) للقرص المصنوع من حديد الزهر ذو الكرافيت المتكور يقع في قيمة متوسطة بين النوعين السابقين. لقد أظهرت النتائج تقارب في القيم الناتجة باستخدام دوال ويبل أحادية التوزيع للبعد ومتعددة التوزيع للأبعاد، لكن الدوال متعددة التوزيع تعطي قيم لاحتمالية الفشل أعلى بقليل من دوال ويبل أحادية التوزيع.